Journal Pre-proof
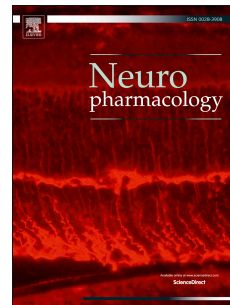
Single-channel mechanisms underlying the function, diversity and plasticity of AMPA receptors

Ian D. Coombs, Stuart G. Cull-Candy

Please cite this article as: Coombs, I.D., Cull-Candy, S.G., Single-channel mechanisms underlying the function, diversity and plasticity of AMPA receptors, *Neuropharmacology* (2021), doi: https://doi.org/10.1016/j.neuropharm.2021.108781.

This is a PDF file of an article that has undergone enhancements after acceptance, such as the addition of a cover page and metadata, and formatting for readability, but it is not yet the definitive version of record. This version will undergo additional copyediting, typesetting and review before it is published in its final form, but we are providing this version to give early visibility of the article. Please note that, during the production process, errors may be discovered which could affect the content, and all legal disclaimers that apply to the journal pertain.

Single-channel mechanisms underlying the function, diversity and plasticity of AMPA receptors

Ian D. Coombs* and Stuart G. Cull-Candy*

Department of Neuroscience, Physiology and Pharmacology,

University College London, Gower Street, London WC1E 6BT, UK

Highlights

- AMPARs have multiple-conductance levels and GluA2 determines channel conductance
- Auxiliary proteins control single-channel properties
- What occupancy-dependent sublevels have revealed about AMPAR operation
- Influence of phosphorylation on AMPAR channel properties and synaptic plasticity
- AMPAR single-channel gating and its multiple modes

*Correspondence: IC (i.coombs@ucl.ac.uk) and SGC-C (s.cull-candy@ucl.ac.uk)

Abstract

The functional properties of AMPA receptors shape many of the essential features of excitatory synaptic signalling in the brain, including high-fidelity point-to-point transmission and long-term plasticity. Understanding the behaviour and regulation of single AMPAR channels is fundamental in unravelling how central synapses carry, process and store information. There is now an abundance of data on the importance of alternative splicing, RNA editing, and phosphorylation of AMPAR subunits in determining central synaptic diversity. Furthermore, auxiliary subunits have emerged as pivotal players that regulate AMPAR channel properties and add further diversity. Single-channel studies have helped reveal a fascinating picture of the unique behaviour of AMPAR channels – their concentration-dependent single-channel conductance, the basis of their multiple-conductance states, and the influence of auxiliary proteins in controlling many of their gating and conductance properties. Here we summarize basic hallmarks of AMPAR single-channels, in relation to function, diversity and plasticity. We also present data that reveal an unexpected feature of AMPAR sublevel behaviour.

Introduction

AMPA receptors (AMPARs) are tetrameric ion channels gated by the central excitatory neurotransmitter glutamate (Traynelis et al., 2010). Unlike NMDA receptors (NMDARs), the AMPARs display rapid kinetics and are thus the primary transduction elements responsible for fast excitatory transmission in the brain. They are also critical in the expression of synaptic plasticity. AMPARs occur in a wide variety of assemblies that differ in their subunit (GluA1-4) composition. Each subunit endows the AMPAR with distinct biophysical, pharmacological and functional properties.

Most native AMPARs are associated with auxiliary transmembrane proteins that increase molecular diversity still further by acting as 'intrusive chaperones' that regulate receptor trafficking (Bats et al., 2007; Tomita et al., 2005b), biogenesis (Schwenk et al., 2019), and channel function. All three 'core' auxiliary subunits, namely transmembrane AMPAR regulatory proteins (TARPs γ2, -3, -4, -5, -7, and -8) (Jackson and Nicoll, 2011; Tomita et al., 2003), cornichons (CNIH2 and -3) (Nakagawa, 2019; Schwenk et al., 2009) and GSG1L (Schwenk et al., 2012; Shanks et al., 2012) influence basic AMPAR single-channel properties.

While functional work on AMPAR channels commenced several decades before information on the receptor's structure was available, molecular and structural studies have cast crucial light on the operation of AMPARs (Chen and Gouaux, 2019; Greger et al., 2017; Hollmann and Heinemann, 1994; Seeburg and Hartner, 2003). To allow us to consider some of the unique functional properties of AMPAR single-channels in a structural context we will therefore first summarize the structural operation of the channel, before focusing on unique functional features revealed by single-channel studies.

1. A brief synopsis of AMPAR operation

AMPARs function as tetrameric assemblies with each subunit consisting of an extracellular N-terminal- and ligand binding domain (NTD and LBD), a transmembrane pore-forming domain (TMD), and an intracellular C-tail (Sobolevsky et al., 2009; Traynelis et al., 2010) (**Fig 1a**). LBDs fold independent of each other forming four freestanding clamshell-like structures, allowing each receptor to bind up to four agonist molecules at any time. The LBD of each subunit connects to the subunit's transmembrane (M1, M3 and M4) domains via three linkers (TM linkers), and it is through these linkers that LBDs control the channel gate. Opening of the gate allows cations to access the conductance pathway and pass through the selectivity filter formed by the M2 re-entrant loop.

Glutamate binds within the angle of the lobes of the LBD, docking *via* its amino and carboxyl groups to the upper D1 lobe (Armstrong and Gouaux, 2000). Once docked, the acidic sidechain group interacts with the lower D2 lobe triggering a large movement of D2 as it encloses the agonist. The LBDs of the four subunits are organized in pairs, interacting with each other through their back-to-back dimer interface (Armstrong and Gouaux, 2000) (**Fig 1a-d**). This rigid arrangement means that LBD closure results in movement of only the D2 lobes, applying tension to their associated TM-linkers which pull the channel open (Chen et al., 2017; Twomey et al., 2017a) (**Fig 1c,e**). Subsequent channel closure occurs either by deactivation (when glutamate unbinds) or *via* desensitization (when glutamate remains bound). During desensitization, the back-to-back interface fractures, the closed LBDs no longer apply tension to the pore linkers, and the pore reverts to its resting (closed) state (Armstrong et al., 2006; Chen et al., 2017; Sun et al., 2002; Twomey et al., 2017b) (**Fig 1d,e**).
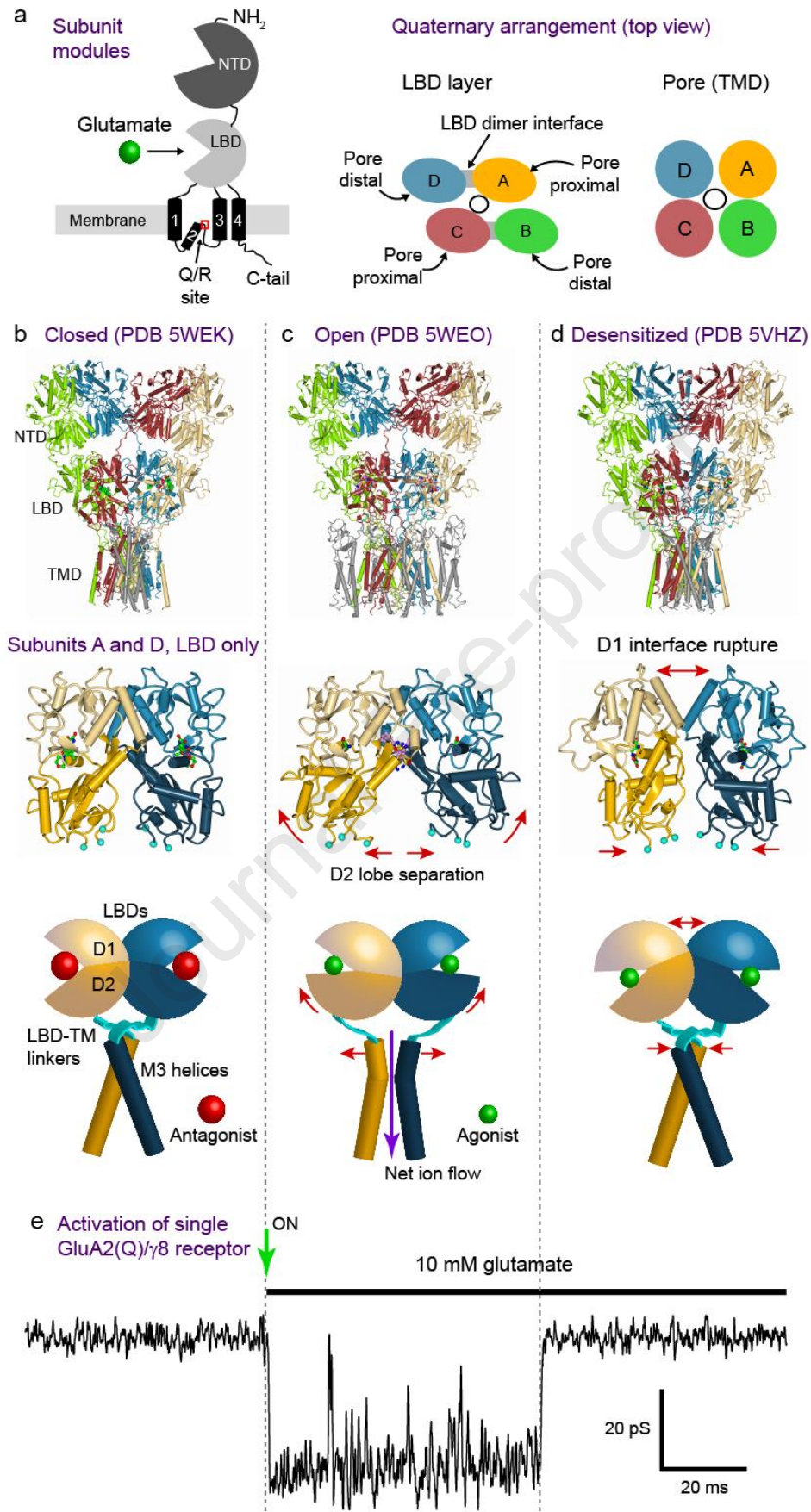
Fig 1. The AMPAR gating cycle and single-channel recording. a) AMPAR subunit topology and modular structure (Left) and the quaternary arrangement and spatial orientation of the LBD and TM

layers around the central axis of the channel (Right). **b**) *Upper row*: Closed channel structure of GluA2(Q)_GSG1L with competitive antagonist ZK200775 bound (GluA2-GSG1L$_{ZK-1}$, (Twomey et al., 2017a)). Each AMPAR subunit is in a different color, the antagonist is shown in green and the auxiliary subunits are shown in transparent gray. *Middle row*: The LBD dimer of subunits 'A' (gold) and 'D' (blue) is shown – upper D1 lobes in pale color, lower D2 lobes in dark color. The LBD junctions of the S1-M1, M3-S2 and S2-M4 linkers are shown as turquoise dots. *Lower row*: Cartoon shows the LBDs, with antagonist ZK200775 (red spheres), TM linkers (turquoise) and the M3 helices. **c**) Same depiction as in b) but for the glutamate and cyclothiazide-bound GluA2(Q)_γ2 open channel structure (GluA2-STZ$_{Glu+CTZ}$ (Twomey et al., 2017a)). Glutamate and cyclothiazide are shown in the structures in green and pink respectively. Glutamate is shown as green spheres in the cartoon. **d**) as in b), but for the closed channel desensitized structure of quisqualate (agonist)-bound GluA2(Q)_GSG1L (GluA2-2xGSG1L$_{Quis}$ (Twomey et al., 2017b)). Quisqualate is shown as green in the structures and cartoon. **e**) Outside-out patch recording of a single GluA2(Q)/γ8 receptor activated by a fast application of 10 mM glutamate. The closed, open and desensitized phases of the response are aligned below their structural correlates. Previously unpublished data, for methods see Coombs et al. (2019).

The closed channel gate is formed by a crossing of the M3 helices towards the extracellular side of the membrane, a structure stabilized by a 'cuff' formed from the short pre-M1 helices (Sobolevsky et al., 2009). Following LBD closure and gate opening, the M3 helix bundle unravels resulting in a large dilation of the central axis, allowing ions access to the channel (Chen et al., 2017; Twomey et al., 2017a). The selectivity filter, located towards the intracellular end of the conductance pathway, is crucial to AMPAR function as it dictates whether the channel has permeability to Ca^{2+} along with Na^+ and K^+. Unlike the other AMPAR subunits, GluA2 is subject to RNA editing which results in the incorporation of a positively changed arginine residue at the tip of the selectivity filter, replacing the genetically encoded neutral glutamine (Sommer et al., 1991). The inclusion of edited GluA2 subunits into the tetramer renders the heteromeric channels Ca^{2+}-impermeable (Hollmann et al., 1991) and abolishes their sensitivity to block by endogenous intracellular polyamines (Bowie and Mayer, 1995; Kamboj et al., 1995; Koh et al., 1995).

2. AMPARs open to multiple-conductance levels

AMPARs possess a panoply of intriguing, and in some cases unique, single-channel properties. The activation of AMPARs gives rise to channel openings characterized by the presence of multiple sub-conductance levels. These events have been described in a wide variety of mammalian neurons and glia (Cull-Candy and Usowicz, 1987, 1989; Howe et al., 1991; Jahr and Stevens, 1987; Smith et al., 2000; Wyllie and Cull-Candy, 1994). The presence of resolvable steps between the various sublevels provided compelling evidence

that the different levels can arise from the same receptor channel (Cull-Candy and Usowicz, 1987, 1989; Howe et al., 1991; Jahr and Stevens, 1987).

It was clear from early studies that individual native AMPA receptor subtypes displayed characteristic 'single-channel signatures'. Thus, two distinct types of multiple conductance AMPAR channel openings were identified in cultured cerebellar granule cells – namely, a channel that opens to 10, 20 or 30 pS, and one that opens to 5 or 10 pS (Wyllie et al., 1993). In addition, a separate population of 'femtosiemens channels' was identified in these cells from noise analysis (~140-360 fS) (Cull-Candy et al., 1988; Smith et al., 2000). By contrast, cerebellar Purkinje cell patches exhibit a different population of multiple conductance AMPAR openings (with discrete sub-conductances of between ~2 -10 pS) (Momiyama et al., 2003). The presence of a variety of distinct multiple conductance AMPAR channels provided early evidence for the idea that a variety of native AMPARs existed within central neurons and glia. This was confirmed by subsequent molecular studies that identified the four homologous AMPAR subunits (GluA1-4), occurring in multiple splice isoforms and able to function as homo- or heteromeric assemblies (Hollmann and Heinemann, 1994; Keinanen et al., 1990).

3. Inclusion of GluA2 affects single-channel conductance

Cloning of the glutamate receptor genes allowed examination of single-channel currents generated by recombinant AMPARs of known subunit composition (summarized in **Table 1**). It is apparent from these studies that AMPAR channel properties depend on subunit composition, RNA editing and splice isoform (Swanson et al., 1997). In particular, AMPAR channel conductance is markedly altered by the presence of GluA2 subunits. Receptors lacking GluA2 are not only calcium permeable but also exhibit a high channel conductance compared with their calcium impermeable counterparts. By contrast, homomeric AMPARs composed entirely of edited GluA2 subunits were found to produce a noise increase rather than resolvable single-channel openings. Fluctuation analysis has revealed the presence of channels with an unusually low (<300fS) conductance. This led to the suggestion that the 'femtosiemens channels' previously detected in cerebellar granule cells could be ascribed to native homomeric GluA2 receptors (Swanson et al., 1997) (see below).

In the majority of single-channel studies on recombinant Ca^{2+}-permeable (CP)-AMPARs, three predominant conductance states of roughly 8, 16 and 24 pS have been resolved (**Table 1**). By contrast, the GluA2 containing Ca^{2+}-impermeable (CI)-AMPARs display openings of predominantly ~10 pS or less. These studies have replicated many of the properties seen with native receptors. Thus, GluA2/4 heteromers display two predominant

6

conductance states of approximately 4 and 9 pS (Swanson et al., 1997), matching reasonably well the 'low conductance' AMPAR channels thought to arise from GluA2 and GluA4 expressing cerebellar granule neurons (Wyllie et al., 1993). Furthermore, homomeric GluA4 receptors display three conductance states of approximately 8, 16 and 23 pS when activated by the full-agonists glutamate or AMPA, resembling the 'high conductance' AMPAR in cultured cerebellar granule cells (Wyllie et al., 1993).

Interestingly, in the study of Swanson et al. (1997), no subunit combination precisely matched the behavior of the native 'high-conductance' cerebellar granule cell channels. For example, while the native channels displayed similar conductance levels in response to both AMPA and kainate (Howe et al., 1991; Wyllie et al., 1993), the recombinant CP-AMPARs (homomeric GluA4) displayed a much lower channel-conductance when activated by kainate rather than AMPA (Swanson et al., 1997). In addition, several studies of cerebellar neurons have identified a population of 40-50 pS channels activated by quisqualate and kainate ((Cull-Candy and Usowicz, 1987; Howe et al., 1991; Smith et al., 2000; Usowicz et al., 1989; Wyllie and Cull-Candy, 1994; Wyllie et al., 1993). Openings to this conductance appear extremely rare or absent in reports from recombinant receptors composed solely of GluA1-4 (**Table 1**).

These apparent discrepancies were largely resolved with the discovery that auxiliary AMPAR subunits such as the TARPs are associated with the majority of native AMPAR complexes (Chen et al., 2000; Schwenk et al., 2014; Schwenk et al., 2012; Tomita et al., 2003). The TARPs increase the efficacy of the partial agonist kainate at AMPARs (Tomita et al., 2005a) helping to explain the occurrence of full conductance openings of native AMPARs elicited by kainate. Furthermore, compared to GluA assemblies in isolation, TARPed AMPARs give rise to a greater proportion of high-conductance openings (Shelley et al., 2012; Tomita et al., 2005a) which can account for the large 40-50 pS openings in native preparations. The presence of TARP γ2 (stargazin) in cerebellar AMPARs can therefore account for the functional mismatch between recombinant GluA4 and native CP-AMPAR channels.

7

Receptor	Agonist	Conductance [pS] (Prevalence [%])				Reference
		Level 1	Level 2	Level 3	Level 4	
Ca²⁺-permeable receptors						
GluA1	Glutamate	7.6 (35)	12.9 (73)	24.8 (34)		(Shelley et al., 2012)
GluA1	Glutamate (2 mM)	5	9	15	24	(Kristensen et al., 2011)
GluA1	AMPA (1 µM) + ctz	10.9	15.2	21.6		(Fucile et al., 2006)
GluA1	AMPA (10 µM)	9.4	13.6	20.5	28.3	(Derkach et al., 1999)
GluA1 + CamKII	AMPA (10 µM)	7.6 (45[a])	12.4 (45[a])	19.3 (55[a])	29.5 (55[a])	(Derkach et al., 1999)
GluA1 + PKA	Glutamate (10 µM)	5(86)	14(12)	20(2)		(Banke et al., 2000)
GluA1 + Calcineurin	Glutamate (10 µM)	4(66)	11(27)	25(7)		(Banke et al., 2000)
GluA2Q	Glutamate	6.1(27)	11.4(53)	18(20)		(Jin et al., 2003)
GluA2Q	Glutamate	6.5(46.7)	14.8(32.4)	23.7(19.1)	36.2(2)	(Zhang et al., 2008)
GluA2Q	Quisqualate (1 mM)	7.5(35.6)	15.4(33.8)	24.2(27.3)	36.8(4)	(Zhang et al., 2008)
GluA2Q	Glutamate (5 mM) + ctz	7.6(19)	15.4(35)	22.8(38)	30.8(7)	(Prieto and Wollmuth, 2010)
GluA2Q	Glutamate (60 µM) + ctz	7.6(43)	15.4(32)	22.8(21)	30.8(4)	(Prieto and Wollmuth, 2010)
GluA2Q	Glutamate	7(71)	14(21)	22(3.5)		(Carrillo et al., 2020)
GluA2Q	Glutamate +ctz	7(4.5)	14(12.5)	22(19)	37(72)	(Carrillo et al., 2020)
GluA3	Glutamate (5 mM) + ctz	10	23	33	47	(Shi et al., 2019)
GluA3	Glutamate (5 mM) + ctz	14	26	39		(Poon et al., 2010)
GluA4	Glutamate (100 µM)	8	15	24		(Swanson et al., 1997)
GluA4	AMPA (10 µM)	7	16	27		(Swanson et al., 1997)
GluA4	Glutamate	8.7(62)	19.5(25)	31(11)	44.8(1)	(Tomita et al., 2005a)
GluA4	Glutamate	8.5(79.4)	18.9(16.4)	29.3(3.2)	40.1(1.0)	(Zhang et al., 2017)
GluA4	Glutamate + ctz	9.6(34.6)	18.0(37.5)	25.6(21.7)	36.3(8.4)	(Zhang et al., 2017)
GluA2Q/4	Glutamate (100 µM)	8	17	26		(Swanson et al., 1997)
GluA2Q/4	AMPA (10 µM)	7	15	24		(Swanson et al., 1997)
With TARPs						
GluA1/γ2	Glutamate	11.5 (32)	22.3(38)	38.8(42)		(Shelley et al., 2012)
GluA1/γ4	Glutamate	12.3 (47)	22.9(33)	42.3(37)	57.2 (9)	(Shelley et al., 2012)
GluA1/γ5	Glutamate	9.4(32)	21.7(61)	38.1(20)		(Shelley et al., 2012)
GluA2Q/γ8	Glutamate	7(3.5)	14(10.5)	22(16)	37(75)	(Carrillo et al., 2020)
GluA2Q/γ2	Glutamate + ctz	3.7	16.1	30.6	38.6	(Coombs et al., 2017)
GluA4/γ2	Glutamate	9.3(42)	21.7(25)	36(24)	49.6(9)	(Tomita et al., 2005a)
GluA4_γ2	Glutamate	9.2	20.3	32	42.8	(Zhang et al., 2014)
Ca²⁺-impermeable receptors						
GluA2/4	Glutamate (100 µM)	4	10			(Swanson et al., 1997)
GluA2/4	AMPA (20 µM)	4	9			(Swanson et al., 1997)
GluA2R/γ2	Glutamate	3.5	6.9	10.3	14.1	(Coombs et al., 2019)

[a] Derkach et al., 2000 reported combined proportions of openings O1/O2 and O3/O4.

Table 1. **AMPARs subunit composition governs single-channel signature.**

Multiple conductance levels identified from single-channel recordings of wild-type AMPAR subunits expressed in HEK293 cells activated by full agonists. Where published, the percentage of openings to each state are displayed in brackets.

4. Auxiliary subunits control single-channel properties

Three families of 'core' transmembrane auxiliary AMPAR subunits appear pivotal in controlling AMPAR behavior. All of the TARPs (γ2, -3, -4, -5, -7, and -8) and two widely occurring members of the cornichon family (CNIH2 and -3) markedly increase single-channel conductance (Coombs et al., 2012; Shelley et al., 2012; Tomita et al., 2005a). Furthermore, by slowing desensitization and deactivation (Cho et al., 2007; Schwenk et al., 2009) they lengthen the duration of single-channel openings (Coombs et al., 2012; Tomita et al., 2005a). In marked contrast, the third type of core auxiliary subunit, GSG1L, decreases the mean single-channel conductance of CP-AMPARs by ~50% (McGee et al., 2015) and reduces excitatory post-synaptic current (EPSC) amplitude in hippocampal neurons (Gu et al., 2016; McGee et al., 2015). Other important families of auxiliary subunits have also been identified, notably the single TM CKAMP/Shisa family (Schwenk et al., 2012; von Engelhardt et al., 2010). These appear to be more peripherally arranged within the AMPAR complex, and their functional effects on single-channel properties seem somewhat less marked. Noise analysis revealed a slight decrease in the single-channel conductance of dentate gyrus granule cell AMPARs from CKAMP44^{-/-} mice (Jacobi and von Engelhardt, 2021; Khodosevich et al., 2014; Klaassen et al., 2016).

As well as dictating the AMPAR current (and thus EPSC) waveform, the auxiliary subunits markedly alter the receptor's pharmacology, and for CP-AMPAR subtypes their susceptibility to block by endogenous and exogenous polyamines (Jackson et al., 2011; Soto et al., 2007). In addition, the auxiliary subunits have a pronounced effect on the receptor's response to low concentrations of glutamate (Coombs et al., 2017; Morimoto-Tomita et al., 2009), and to high frequency activation (Carbone and Plested, 2016). Thus, the discovery that auxiliary subunits are crucial in AMPAR functioning has radically altered our understanding of AMPAR single-channel behavior. Nonetheless, while in total there are at least 15 transmembrane AMPAR auxiliary proteins that could assemble with, and potentially modify the functional properties of, AMPAR complexes, many of these AMPAR auxiliary subunit combinations are yet to be examined at the single-channel level (**Table 1**).

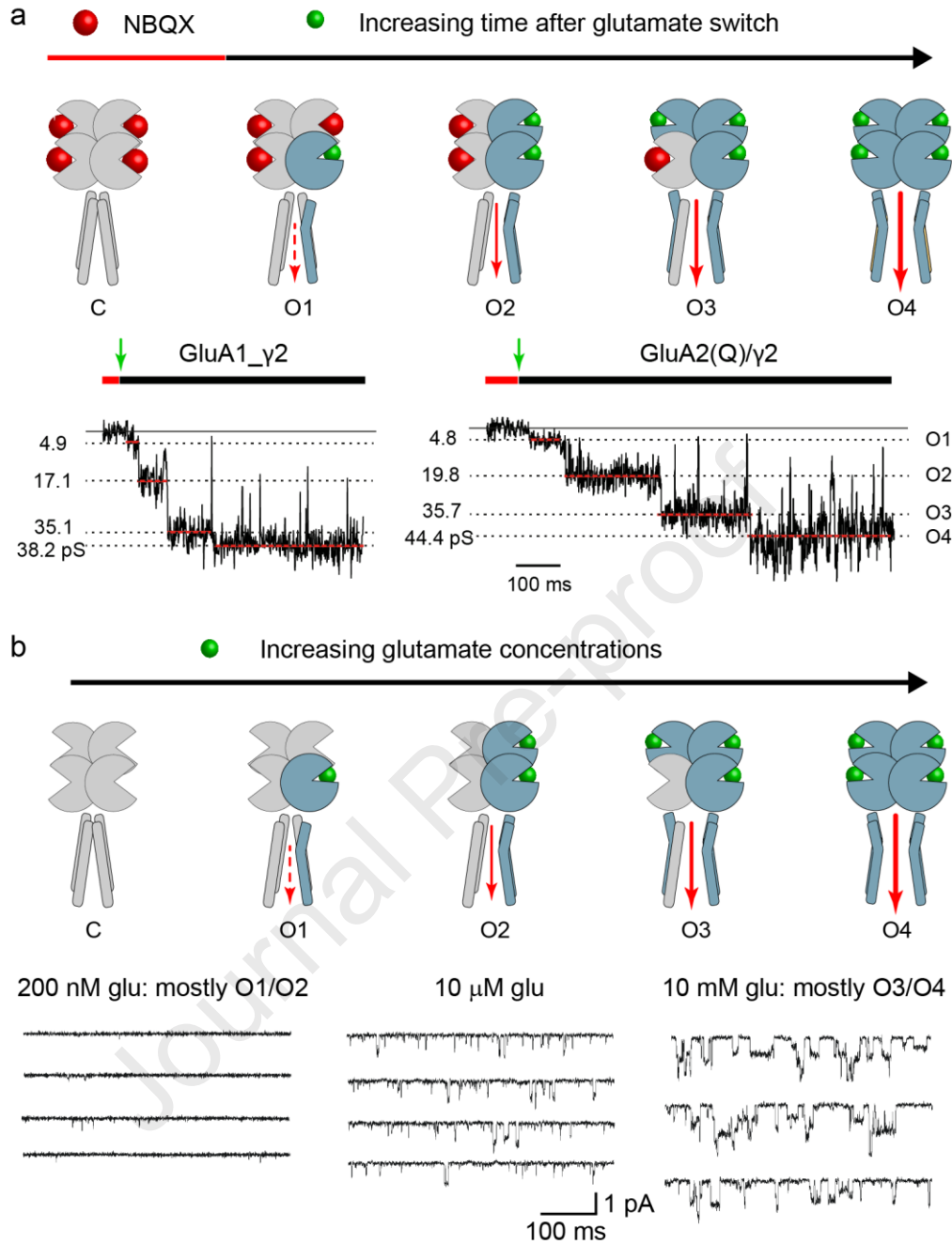## 5. What has the analysis of sublevels revealed about AMPAR function?

The presence of sub-conductance states is a feature that is particularly striking in AMPARs and the analysis of these has revealed surprising and unique features of the binding-gating mechanism associated with channel activation.

Sublevels reflect the level of agonist occupancy of LBDs: The binding of glutamate and the subsequent channel gating occur on a fast timescale – typically with current rise times of

200-400 μs. However, the unbinding of competitive antagonists such as NBQX (2,3-dioxo-6-nitro-1,2,3,4-tetrahydrobenzo[f]quinoxaline-7-sulfonamide) is several orders of magnitude slower (MacLean et al., 2014; Rosenmund et al., 1998). Thus, by saturating receptors with NBQX before fast application of an agonist, the time course and process of single-channel activation can be directly resolved over a period of hundreds of milliseconds as the NBQX molecule bound to each LBD is replaced by glutamate (Coombs et al., 2017; Rosenmund et al., 1998) (**Fig 2a**).

Using this elegant approach, Rosenmund et al. (1998) found that when occupied by a single agonist molecule (plus 3 NBQX molecules) homomeric GluA3 or chimeric AMPA-/kainate (GluA3/GluK2) receptors did not generate a detectable conductance. By contrast, the binding of two agonist molecules produced a small current that increased in a stepwise fashion as the third and fourth agonist molecules bound (Rosenmund et al., 1998). This picture is consistent with the view that channel conductance increases as more LBDs become occupied by the agonist. Hence, the maximum conductance arises only from a fully saturated AMPAR. These experiments provided the first mechanistic insight into the origin of sublevel behavior of AMPARs, and suggested that sublevels reflected a novel graded response to increased agonist occupancy.

Single-channel conductance depends on agonist concentration: If AMPAR sublevel behavior does indeed reflect the level of agonist occupancy, one would predict that single-channel conductance would display agonist concentration-dependence. While the steady-state application of different glutamate concentrations does not allow sublevels of known occupancy to be examined, it provided a direct test of the idea that low glutamate concentrations, and hence less occupied receptors, generate a skew towards lower conductance states. Indeed, single AMPAR channels from cerebellar granule cells (Smith and Howe, 2000) and hippocampal CA1 pyramidal cells (Gebhardt and Cull-Candy, 2006) displayed an increased prevalence of low conductance openings in micromolar and submicromolar glutamate (when compared with mM levels). Furthermore, as expected, the amplitude of the individual sub-conductance levels was concentration independent (**Fig 2b**). Additionally, at low glutamate concentrations the openings displayed short open periods (Gebhardt and Cull-Candy, 2006) and a low P_{open} (Smith and Howe, 2000). A similar trend was also apparent in recombinant GluA2(Q) receptors recorded with 60 μM or 5 mM (saturating) glutamate (Prieto and Wollmuth, 2010) (see **Table 1**).

Fig 2. AMPAR sublevels represent agonist occupancy of four LBDs.

a) Cartoon showing how glutamate occupancy and channel gating is slowed by prior application of the competitive antagonist NBQX. Lower panels show recordings from individual TARPed AMPARs. As glutamate replaces NBQX, the channel opens in a stepwise manner, revealing four occupancy-dependent conductance levels in these TARPed AMPARs. Adapted from Coombs et al. (2017). **b**) Cartoon depicting increasing LBD occupancy with glutamate concentration. Unoccupied subunits are shown as gray, occupied subunits are blue. Lower panel shows single-channel currents recorded in an outside-out patch from a hippocampal CA1 neuron exposed to the three different concentrations of glutamate (200nM, 10µM, 10mM). Note that the proportion of high-conductance openings increases with glutamate concentration. Adapted from Gebhardt and Cull-Candy (2006).

11

Together with the observation that the conductance of single-channels is concentration-dependent, the stepwise time-course of single-channel openings during NBQX unbinding provides compelling support for the view that the AMPAR's LBDs contribute to channel opening in a cumulative fashion. Mechanistically, the closure of each LBD is believed to pull on the linkers connected to the pore. Therefore, it seems that individual LBD closures influence the pore in a concerted manner, to progressively ratchet the pore to its fully open state. It has been proposed that variable sidechain orientation at the Q/R site may also play a key role in giving rise to different conductance sublevels (Twomey et al., 2017a). This latter idea is difficult to test directly, but may be amenable to molecular dynamics simulations.

Despite the broad structural similarities among iGluRs (Traynelis et al., 2010), the occupancy-dependent gating behavior of the AMPARs appears quite distinct. Kainate receptors display sublevels that depend weakly, or not at all, on agonist concentration, suggesting a strong degree of cooperation between subunits (Smith and Howe, 2000). Meanwhile NMDARs require both GluN1 subunits to be occupied by glycine, and both GluN2 subunits to be occupied by glutamate for concerted channel opening (Patneau and Mayer, 1990). Thus, the ratcheting type arrangement that prevails at AMPARs appears unique amongst the iGluR superfamily. Indeed, no other ligand gated ion channel has so far been described with a channel conductance that is concentration dependent.

6. TARPs modify sub-conductance gating and channel operation

Binding of a single agonist molecule is sufficient to partially open the channel: We recently examined NBQX unbinding from TARPed AMPARs (GluA1 and GluA2(Q) with γ2). In contrast with TARPless receptors, four sequential conductance states could be resolved in the presence of γ2, suggesting that in this case the binding of a single agonist molecule allows partial opening of the AMPAR pore (Coombs et al., 2017). This finding is in keeping with earlier observations that γ2 increases agonist efficacy. Thus, macroscopic data has shown an increase in efficacy of the partial agonist kainate (Tomita et al., 2005a), and conversion of CNQX from an antagonist to a partial agonist (Menuz et al., 2007). Singly-liganded gating can also help explain the bell-shaped steady-state dose response relationships displayed by AMPAR/TARP complexes in certain conditions (Morimoto-Tomita et al., 2009), as singly-liganded receptors are gated, but are subject only to limited desensitization when TARPed (Coombs et al., 2017).

12

TARPed AMPARs exhibit increased mean single-channel conductance: The amplitude of the full- and sub-conductance levels measured during NBQX unbinding appear larger with γ2-associated AMPARs than receptors in the absence of a TARP. We measured values of 4, 16, 31 and 39 pS for receptors associated with γ2 (Coombs et al., 2017), whereas GluA3 and GluA3/GluK2 chimeras in the absence of a TARP gave values of 0, 5, 15 and 23 pS (Rosenmund et al., 1998). This is consistent with the identification of unique high conductance states of certain AMPAR/TARP combinations (Shelley et al., 2012), but, at face value, is at odds with the idea that the sub-conductance levels of TARPed and TARPless receptors are identical, and that TARPs act simply to increase the relative proportion of higher conductance openings (Tomita et al., 2005a). However, one caveat is that the single-channel behavior of partially glutamate-occupied receptors (where the remaining LBDs are either unoccupied or NBQX-bound), is not necessarily equivalent. For example, the relative mobility of LBD conformations is more restricted when bound by an antagonist (Plested and Mayer, 2009) – a feature that could result in Apo and NBQX-bound LBDs influencing the pore in subtly different ways. Further, in the absence of TARPs certain AMPARs can display single-channel openings of >30 pS (**Table 1**) (Carrillo et al., 2020; Poon et al., 2010; Prieto and Wollmuth, 2010; Shi et al., 2019; Tomita et al., 2005a; Zhang et al., 2017). Hence, it seems that higher conducting states are not exclusive to TARPed receptors. The exact nature of the influence of TARPs on AMPAR single-channel conductance sublevels therefore remains an open question.

7. Do channel gating properties depend on position of occupied subunits?

Open channel structures of homomeric TARPed GluA2 AMPARs have been determined from either a tandem construct for GluA2(Q) and γ2 (GluA2Q-STG) (Twomey et al., 2017a), or separately expressed GluA2(R) and γ2 (GluA2-TARP γ2) (Chen et al., 2017). As expected, in both open channel structures the narrowest point of the pore is no longer the activation gate formed by the M3 helixes, rather it is at the level of the selectivity filter and pore loop. As GluA2 was fully occupied with agonist in both these studies, the structures seem likely to correspond well to the channel's maximum conductance state (O4). Of note, the structures are asymmetrically open. In other words, LBD closure within the distal B/D subunits (see **Fig 1**) produces greater separation of the channel regions than seen for LBD closure within the proximal A/C subunits.

The structures of the open AMPAR channels raise an important question regarding the nature of sub-conductance states. For partially occupied channels, given that the B/D subunits produce more separation than the A/C subunits (with the Cα separation of B/D Thr625 being approximately double that of A/C Thr625 in all structures), does the

13

proximal/distal positioning of the closed LBDs influence the single-channel conductance of the open channel? Evidence from NMDARs suggests that the distal GluN2 subunits transmit more energy at an earlier stage of gating than the proximal GluN1 subunit (Kazi et al., 2014). Therefore, it seems feasible that glutamate binding to the proximal rather than the distal AMPAR subunits can produce different functional outcomes. Indeed, a recent structure of an activated GluA1/2/γ8/CNIH2 assembly showed that the A/C GluA1 subunits and B/D GluA2 subunits have disparity in their separation virtually throughout the entire pore, including the selectivity filter (Zhang et al., 2021).

One possible outcome of the dependence of gating on the position of the occupied subunits is that receptors with the same numerical occupancy could display different functional properties, including distinct sublevel conductances. In **Fig 3a** we display the aligned pore-forming regions of cryo-EM structures of GluA2Q in agonist-bound activated and antagonist-bound closed conformations, visualized as partially gated 'structural chimeras'. Given the relatively increased separation of the distal B/D subunits compared with the proximal A/C subunits, the bi-liganded structural chimeras clearly show different degrees of pore dilation, which may influence channel conductance. Interestingly, our NBQX-unbinding data for single AMPAR/γ2 combinations (Coombs et al., 2017) contains some support for the idea that gating of proximal vs distal subunits differs functionally. By counting back from O4 to O1 in the 'staircase' of open states, we can unambiguously pinpoint the O2 state in a majority of sweeps (see **Fig 3b**). Identified in this way, the O2 openings showed a mean conductance of 16.1 pS. However, the amplitude distribution displayed a standard deviation of fitted conductances that was visibly greater than that seen for other open levels (**Fig 3b,c**). Our analysis indicates that openings to O2 are better approximated by a two-component fit containing a 7.4 pS component (30% of total) and a 19.4 pS component (70%) (**Fig 3c**). Given the relative proportions of these O2 openings, we posit that the smaller component arises from receptors gated by the two proximal (A/C) subunits. Structurally these are predicted to have reduced dilation of the gate, and hence, potentially, a lower conductance (**Fig 3a**). They are expected to give rise to ~25% of all O2 openings – strikingly similar to the proportion we have observed. This unexpected feature of AMPAR single-channel behavior ties in neatly with the structural findings.
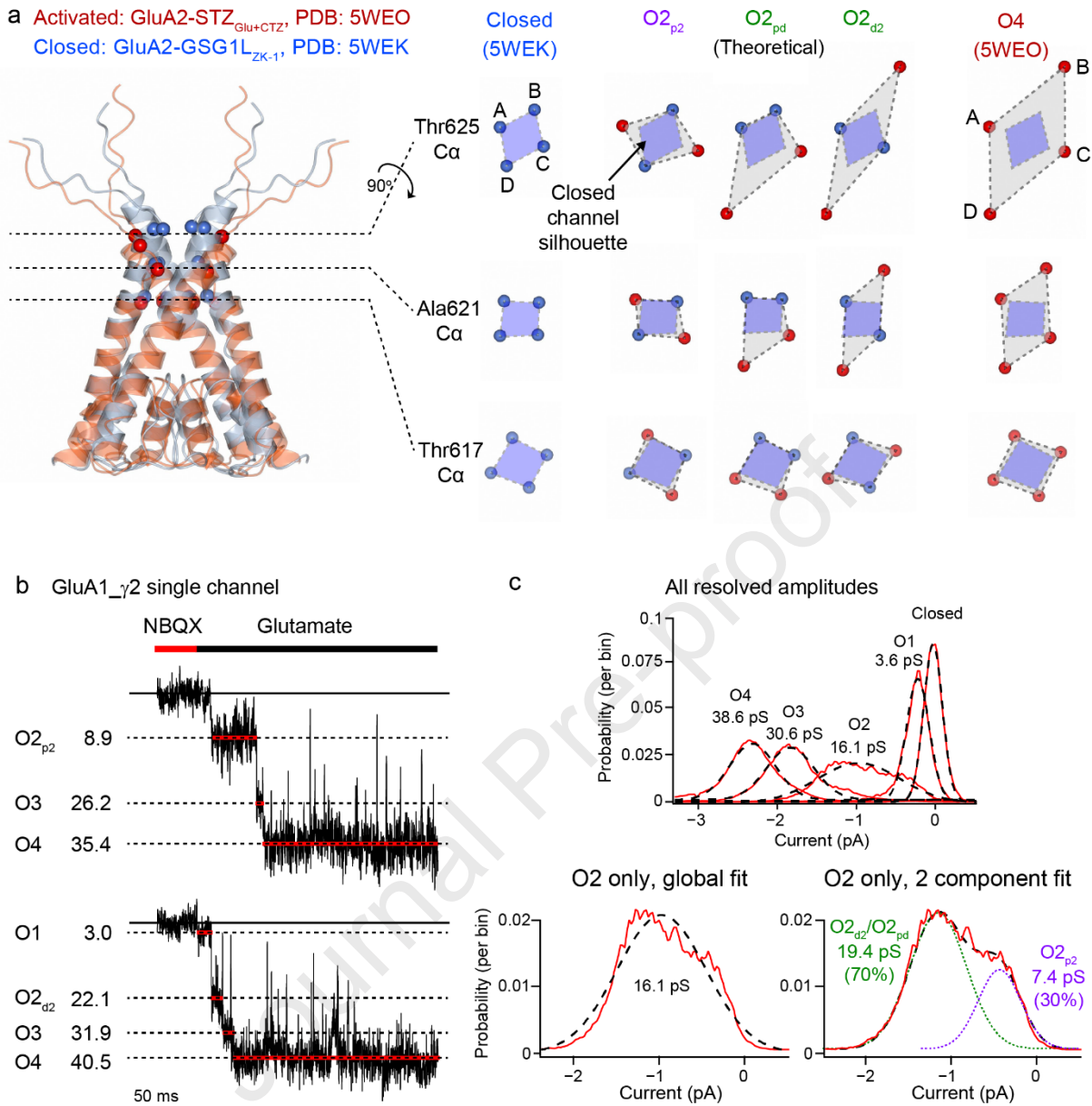
Fig 3. Structural modelling and single-channel recordings reveal that O2 openings may contain more than one conductance level.

a) *Left*. The aligned M2, M3 and M3-S2 linker regions of closed (blue) and activated (red) structures of GluA2Q_auxiliary subunit tandem constructs (Twomey et al., 2017a). *Right*. Top-down views of the gate region showing the Cα atoms of Thr617, Ala621 and Thr625 for the pore proximal (A and C), and pore distal (B and D) subunits of the closed (left) and fully open (right, O4) structures. Models of three 'half-occupied' (two LBDs occupied) channels (middle) were constructed using only two gated subunits (O2$_{p2}$ both proximal; O2$_{pd}$, one proximal, one distal; and O2$_{d2}$ both distal). The blue shaded area corresponds to the closed channel dimensions at each level, and the silhouette of this area is superimposed on the other structures. Note how the area of dilation (gray) of O2$_{p2}$ is markedly smaller than O2$_{pd}$ and O2$_{d2}$, suggesting they may be functionally different. **b**) Representative records from a single-channel GluA1_γ2 outside-out patch in the continuous presence of 50 µM cyclothiazide, jumped from 50 µM NBQX into 10 mM glutamate. Data from Coombs et al. (2017). The upper patch (which does not display a measurable O1 state) displayed a smaller conductance O2 opening (potentially O2$_{p2}$). The lower patch displayed all four sequential sublevels (O1-O4) including a larger

15

conductance O2 opening (potentially $O2_{d2}$). **c**) *Upper*. Histogram showing all resolved openings with their designated conductance level. From Coombs et al. (2017). O2 openings showed a wide distribution that can either be fitted with a single component (lower left) or a double component (lower right). The double peak suggests that O2 openings can represent two conductance levels, the smaller of which may correspond to $O2_{p2}$ as it comprises roughly one quarter of the events. For methods see Coombs et al. (2017).

8. Non-competitive antagonists influence sub-conductance behavior

While competitive blockers directly influence the number of glutamate molecules bound to the receptor, non-competitive ones such as perampanel (Hibi et al., 2012) and GYKI-52466 (Donevan and Rogawski, 1993) inhibit AMPAR currents even when receptors are fully glutamate-saturated. Crystallographic data show that at saturating concentrations perampanel molecules bind to the receptor at the interface between the ion channel and the linkers connecting it to the LBD. By binding to the pre-M1, M3 and M4 helices, each of the four perampanel molecules additionally form a single contact with the M3 helix of an adjacent subunit (Yelshanskaya et al., 2016). The location of the binding pocket therefore makes it likely that perampanel mediates inhibition through the TM-LBD linkers, by acting as a 'wedge' that prevents ligand binding being converted into the movement of subunits needed for channel opening.

At the single-channel level, for concentrations producing partial block, non-competitive antagonists could act by decreasing channel open probability, reducing the amplitude of each sub-conductance state, or lowering the relative proportion of channels that open to the larger conductance levels. Given that the binding of each drug molecule is contained largely within a given subunit, one might predict that the affected subunit could no longer contribute to gating, and hence that the receptor would be unable to open to its maximum conductance. However, as the subunits without drug bound should still contribute to channel gating, the amplitude of sub-conductance levels would be unaffected. Broadly speaking, these predictions have been borne out by single-channel recordings of GluA3 receptors made in the presence of 2 μM perampanel ($\sim IC_{50}$) (Yuan et al., 2019). The channel open probability was reduced from 0.96 to 0.77; the incidence of O3 and O4 openings was reduced to negligible levels, whilst the conductance amplitude of O1 and O2 was left unchanged. These results add further support to the idea that each AMPAR subunit contributes independently to increase the single-channel conductance.

By contrast, Shi et al. (2019) found that GYKI-52466 produced channel behavior that was markedly different from that seen with perampanel and altogether more surprising. In the majority of single-channel patches exposed to 10 μM GYKI, GluA3 receptors opened to only a single conductance level – which in some cases lasted for tens of minutes. This suggests

that GYKI-52466 binding produces a strong coupling between subunits such that the receptor can no longer display the rapid transitions between sublevels indicative of independent LBD closures. Shi et al. (2019) proposed a model whereby the two-fold symmetry of the LBD-TM linkers would allow low concentrations of modulators such as GYKI to bind preferentially to just two of the four AMPAR subunits. It was suggested that, while this could block the gating motions of the TM-linkers in the bound subunits, the small interaction of GYKI-52466 with the adjacent M3 region could simultaneously stabilize the linkers of the neighboring subunits that are not bound by blocker, leading to long-lived open conformations.

9. Homomeric GluA2 gives rise to conducting desensitized channels

Our recent experiments cast unexpected light on the origin of the femtosiemens AMPAR channels previously identified in cerebellar neurons and in HEK cells expressing recombinant homomeric Q/R edited GluA2 receptors (Cull-Candy et al., 1988; Swanson et al., 1997). We found that homomeric GluA2(R)/γ2 receptors display unusual properties, principally a large steady-state conductance and non-parabolic current-variance relationship (Coombs et al., 2019). To dissect the mechanism underlying this unusual behavior, we examined recordings from patches that contained around 3-6 receptors so both single-channel openings and macroscopic behaviours could be observed in the same records (**Fig 4**). Although the cells expressed a homogeneous population of GluA2(R)/γ2 AMPARs, our analysis revealed the presence of two distinct types of channel openings during 100 ms glutamate applications. Glutamate activated currents consisted of a burst of single-channel openings with conductances in the same range as those arising from other CI-AMPARs - roughly ~4 -14 pS (Coombs et al., 2019). However, these directly resolved openings were superimposed on a steady-state current mediated by channels with an estimated unitary conductance of ~670 fS. Our experiments indicated that these 'femtosiemens' events arose from a conducting desensitized state of the homomeric GluA2(R)/γ2 receptors.

Fig 4. Single-channel recordings identify two distinct classes of GluA2(R)/γ2 openings.

a) GluA2(R)/γ2 currents from an outside-out patch containing few channels (–60 mV). Forty consecutive applications of 10mM glutamate (gray bar) are overlaid. Note that despite the small number of channels, there are no sojourns to baseline suggesting homomeric GluA2 receptors do not fully close in the continued presence of glutamate, **b**) Individual responses exhibiting discrete channel openings (black arrows) superimposed on a persistent steady-state low noise current. Note the decay of the steady-state current on glutamate removal (gray arrows) is slow/exponential as it reflects closure of multiple low conductance (femtosiemens) channels. **c**) Histogram of channel conductance for all resolvable single-channel openings. **d**) Cartoon representation of the femtosiemens openings which underlie the large steady-state currents seen. GluA2(R)/γ2 channels bind glutamate (gray spheres), closing the clamshell LBDs and opening the pore to the full (picosiemens) open channel conductance. Desensitization does not fully close the pore, leaving a conductance around one tenth of the open channels (in the femtosiemens range). Adapted from Coombs et al. (2019).

Cryo-EM data suggest the desensitized GluA2(R)/γ2 pore is closed (Chen et al., 2017). So, how might ions flow through these channels? Given the clear functional difference between edited and unedited GluA2, the Q/R site must hold the key. In homomeric GluA2(R) receptors, all four pore-loop arginines are in close proximity at the selectivity filter that is thought to form a "lower gate" (Twomey et al., 2017a). An attractive possibility is that

18

following desensitization repulsion of the four positive arginines inhibits full closure of this gate, allowing ions to continue flowing but at a reduced rate. Further, Q/R editing can directly influence the M3 region (Wilding et al., 2010) so this repulsion may also potentially impact closure of the 'upper' M3 gate. Nonetheless there is clear disparity between the functional and structural data which remains unexplained. Of note, although homomeric GluA2(R) receptors were previously suggested to display chloride permeability (P_{Cl}/P_{Cs} = 0.19, Burnashev et al. (1996)), we found no evidence for this in the TARPed GluA2(R)/γ2 receptors (Coombs et al., 2019). Hence, the femtosiemens conductance does not reflect a chloride current.

It was previously suggested that AMPARs rarely assemble as homomers of GluA2 as heteromerization with subunits GluA1, 3 and 4 was preferred (Greger et al., 2003; Rossmann et al., 2011; Zhao et al., 2012). However, there is more recent structural evidence for the presence of homomeric GluA2 receptors within the CNS (Zhao et al., 2019), a finding that makes the behavior of TARPed homomeric GluA2(R)/γ2 receptors particularly intriguing. More than half of their steady-state current is carried by desensitized receptors (Coombs et al., 2019). Hence, this novel form of gating could make a substantial contribution to synaptic currents during high frequency activity, at sites that have slow transmitter clearance, or where extrasynaptic receptors that are liable to be activated by transmitter spillover. As AMPAR subunits consist of a dimer of dimers in the LBD layer, the presence of conducting desensitized GluA2(R)/γ2 channels raises a question relevant to AMPARs of any composition. Does the rupturing of just one LBD dimer result in a fully desensitized receptor? It might perhaps be expected that a fully occupied receptor with a single ruptured LBD dimer would generate openings that resembled the O2 state. Indeed, kinetic modelling of the recovery from desensitization of macroscopic homomeric GluA1 responses (Bowie and Lange, 2002) required the presence of conducting desensitized states to explain the early time course of the recovery and the rates of re-entry into desensitization. Interestingly, these models predicted a conductance in the femtosiemens range for partially desensitized TARPless and unedited receptors. Thus low conductance desensitized channels may be a feature of other native AMPAR combinations independent of Q/R editing.

10. Phosphorylation influences synaptic strength by altering channel properties

In hippocampal neurons phosphorylation of GluA1 dictates receptor surface trafficking (Esteban et al., 2003; Hayashi et al., 2000; Lee et al., 2003), (but see Diaz-Alonso et al., 2020), and in recombinant systems, phosphorylation of GluA1 increases the amplitude of single-channel currents (Banke et al., 2000; Derkach et al., 1999). Hence, AMPAR phosphorylation is thought to produce rapid changes in the amplitude of AMPAR currents

and play a key role in plasticity changes such as long-term potentiation (LTP) (Diering and Huganir, 2018).

CaMKII phosphorylation of GluA1: For many ionotropic receptors their activation is thought to involve a simple two-step sequential reaction of agonist binding followed by channel gating (Del Castillo and Katz, 1957). At the level of the individual subunit it is likely that AMPARs follow this type of sequential reaction scheme. Hence, while a high concentration of glutamate will facilitate the binding step, the next step (D2 closure) is independent of concentration and reflects coupling efficiency (efficacy) (**Fig 5a**). For fully occupied receptors, those with a high coupling efficiency will display conductance states of mainly O3 and O4, while receptors with a low coupling efficiency will open predominantly to lower conductance levels (**Fig 5b,c**). Therefore increasing or decreasing coupling efficiency has the potential to control the magnitude of AMPAR currents, and hence of synaptic strength.

Phosphorylation of GluA1 Ser831 by Ca^{2+}/calmodulin-kinase II (CaMKII) (Barria et al., 1997) enhances the relative proportion of large conductance single-channel openings by increasing coupling efficiency (Derkach et al., 1999) (**Fig 5c**). As expected, the phosphomimic mutations S831D (Derkach et al., 1999) and S831E (Kristensen et al., 2011) also increase mean channel conductance, while a mutant that is resistant to phosphorylation, S831A, has the opposite effect (Kristensen et al., 2011). Noise analysis has identified a similar, but non-additive effect of phosphomimic mutations at two further positions (Ser818 and Thr840) within GluA1's C-tail (Jenkins et al., 2014). While the latter two sites are not thought to be targets of CaMKII, all three residues (Ser818, Ser831 and Thr840) are targets of PKC (Lee et al., 2007; Lin et al., 2009; Roche et al., 1996). Thus PKC activation is anticipated to enhance coupling efficiency of GluA1, while dephosphorylation (as seen at Thr840 with protein phosphatase 1/2A) is expected to decrease it (Gray et al., 2014).
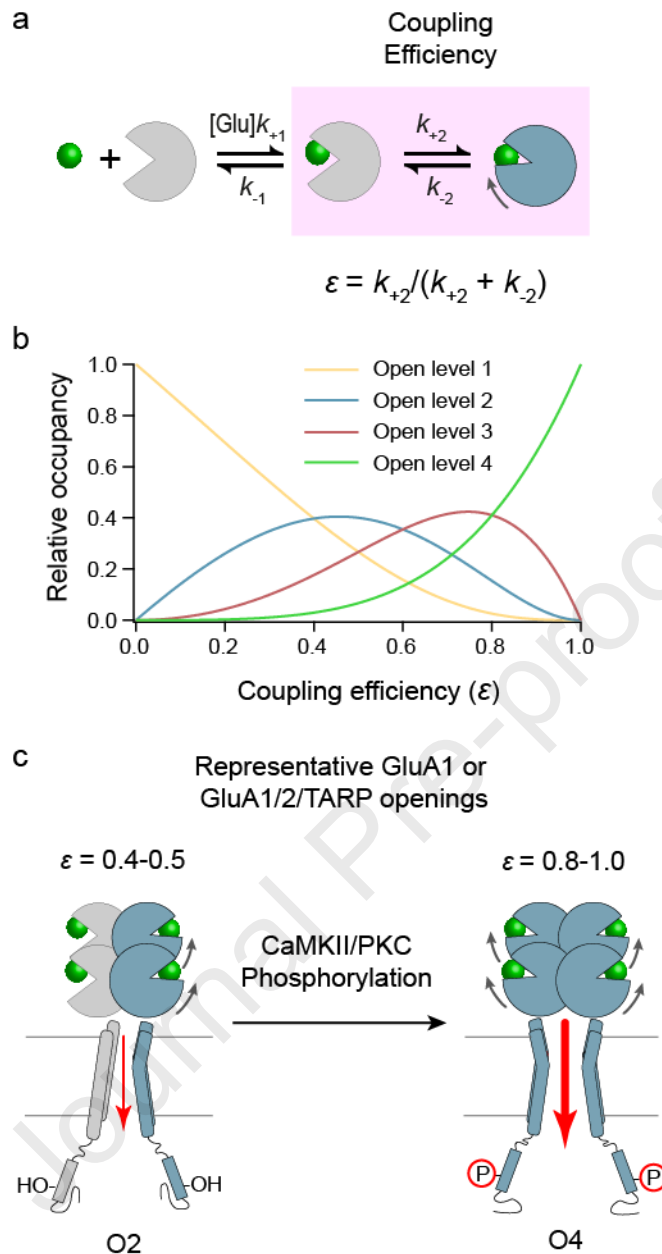
20

a

Coupling
Efficiency

$$\varepsilon = k_{+2}/(k_{+2} + k_{-2})$$

b

c

Representative GluA1 or
GluA1/2/TARP openings

$\varepsilon = 0.4$-0.5

$\varepsilon = 0.8$-1.0

CaMKII/PKC
Phosphorylation

O2

O4

Fig 5. Likelihood of LBD closure – coupling efficiency – controls channel conductance and is modulated by phosphorylation.

a) Agonist binding and LBD closure comprise a two-step process. Following binding of glutamate to the upper lobe, the relative likelihood of LBD closure (the coupling efficiency, ε) will be dictated by the rates of LBD closure (k_{+2}) and LBD opening (k_{-2}) (adapted from (Kristensen et al., 2011)). **b**) Graph illustrating how coupling efficiency affects the theoretical relative occurrence of the four different open channel sublevels. Adapted from Shelley et al. (2012). **c**) Phosphorylation of GluA1 by CaMKII at Ser831, or by PKC at Ser818, Ser831 and/or Thr840 elevates the coupling efficiency from roughly 0.5 to nearly 1, increasing the prevalence of larger conductance openings. A similar mechanism likely underlies the increase in conductance of GluA1/2/TARP complexes following GluA1 Ser831 phosphorylation.

21

Structural analysis combined with single-channel studies has suggested that the extent of LBD closure is a major determinant of agonist efficacy. Thus partial agonists cause the LBD to adopt a lower degree of domain closure than seen with full agonists (Armstrong and Gouaux, 2000; Jin et al., 2003). This correlates with a reduced proportion of high conductance openings, even at a saturating concentrations of the partial agonist (Jin et al., 2003). As with glutamate, the coupling efficiency of partial agonists acting on GluA1 is increased by CaMKII (Kristensen et al., 2011). Indeed, the coupling efficiency of the partial agonist willardiine, is enhanced in phosphorylating conditions to the level seen with glutamate in basal conditions ($\varepsilon \sim 0.4$, Kristensen et al. (2011)). Taken together, GluA1-Ser831 phosphorylation reduces the energy needed for individual subunits to undergo gating transitions, which will allow fast acting enhancement of synaptic responses following activation of CaMKII and PKC.

PKA phosphorylation of GluA1: Phosphorylation of GluA1 Ser845 also increases AMPAR responses, in this case by increasing the receptor channel's peak open probability (Banke et al., 2000). In contrast with Ser831, phosphorylation of Ser845 did not alter single-channel conductance, mean channel open period, or burst length. To account for this, Banke et al. (2000) proposed a model in which the receptor can reside in two states - one permissive to channel opening and the other non-functional. By shifting the balance between these states, the response of a population of GluA1 receptors to fast or synaptic applications of glutamate can be enhanced by PKA phosphorylation and reduced by calcineurin dephosphorylation of GluA1 Ser845 (Banke et al., 2000).

11. Interplay between TARPs and phosphorylation in AMPAR plasticity

GluA1/2 heteromers play a central role in expression of LTP at hippocampal CA1 synapses (Shi et al., 2001). Exogenous application of activated CaMKII to hippocampal AMPARs increases their conductance (Kristensen et al., 2011), as first described for phosphorylation of recombinant GluA1 homomers (Derkach et al., 1999). However, in marked contrast, CaMKII phosphorylation of recombinant heteromeric GluA1/2 receptors gives no such conductance increase (Kristensen et al., 2011; Oh and Derkach, 2005). This striking disparity between the native and recombinant forms of GluA1/2 reflects the fact that native AMPARs in CA1 cells are associated with TARPs. Thus, GluA1/2 receptors that contain GluA1 phosphomimic S831E exhibit a larger conductance than those that contain GluA1 phospho-lacking S831A - but only in the presence of TARPs (γ2 or γ8; (Kristensen et al., 2011)).

The mechanism by which TARPs allow increased coupling efficiency of GluA1/2 heteromers following phosphorylation of their GluA1 subunits is unclear. However, it is notable that the enhanced proportion of higher conductance homomeric GluA1 sublevels that occurs in the presence of TARPs, is boosted still further by CaMKII phosphorylation, so the effects are cumulative (Kristensen et al., 2011). It is not known for homomeric GluA1 channels, whether the peak open probability that is enhanced by co-assembly with TARPs (Coombs et al., 2012) is further increased by phosphorylation of Ser845. These effects might occlude each other (see Kristensen et al. (2011)). However, for hippocampal CA1 AMPAR assemblies that are expected to be mediated mainly by GluA1/2 heteromers associated with TARP γ8 and CNIH2 (Yu et al., 2021), the peak open probability is sensitive to phosphorylation: ~0.92 in the presence of activated PKA *vs* ~0.39 in the presence of calcineurin (Banke et al., 2000). This is consistent with the view that the phosphorylation state of Ser845 influences synaptic transmission in hippocampal CA1 neurons and is therefore important in LTP expression.

Structural basis for phosphorylation-mediated modification of channels: The data described above reveal that there are at least three functionally distinct phosphorylation forms of the GluA1 C-tail: unphosphorylated, Ser831 phosphorylated, and Ser845 phosphorylated. There are presumably structural distinctions between these forms. However due to the high degree of disorder in the intracellular C-tail regions of AMPARs, these have not so far proved amenable to crystallographic or cryo-EM analysis. Nonetheless, molecular modelling has identified the potential for limited secondary structure within the membrane proximal GluA1 C-tail, and NMR spectra have confirmed the presence of an alpha helix within the vicinity of Ser831 (Jenkins et al., 2014). Further, the phosphorylation state of Ser831 was found to influence the signature of this helix. By contrast, Ser845 phosphorylation did not appear to form part of, or to influence, any secondary structural elements. This would suggest that the effects of Ser831 (but not Ser845) phosphorylation are mediated by perturbations of local secondary structure.

It is unclear how conformational changes of the C-tail are able to feedback and influence channel properties. However, as the C-tail links directly to the M4 helix, it is tempting to speculate that phosphorylation mediated changes are transmitted via M4 to the channel pore or even to the LBD-TM linkers, to produce a functional outcome. Indeed, despite being peripheral to the conductance pathway, the M4 domain can exert a profound influence on iGluR receptor currents (Amin et al., 2018). Phosphorylation of individual AMPAR subunits has the potential to alter interactions of the C-tail that occur both within and between subunits of the same receptor assembly, with other intracellular protein partners or indeed

23

the plasma membrane. These interactions might in turn place constraints on M4 that alter LBD coupling efficiency or channel open probability.

It is also worth noting that GluA1's M1-M2 intracellular loop is strongly electronegative, while its C-tail carries a net positive charge. A charge-mediated interaction that can be altered by phosphorylation would have the potential to modify receptor properties. It is therefore possible that the effects of phosphorylation on receptor properties are mediated by the intracellular portion of the pore. Indeed, we previously demonstrated a crucial role of GluA1 Asp586 (the Q/R +4 site) in mediating the effects of TARPs on AMPAR single-channel conductance (Soto et al., 2014). When Asp586 was neutralized (D586N), GluA1 co-expression with γ2 or γ3 no longer increased single-channel conductance. And when the charge was reversed (D586K), TARP co-expression decreased single-channel conductance. Given the role of this site in TARP-dependent conductance changes, and the fact it is accessible from the cytoplasm, it is also possible that the pore loop is involved in mediating the phosphorylation-dependent changes in GluA1 single-channel properties.

12. The relevance of multiple modes of AMPAR single-channel gating

Activation of AMPARs by sub-saturating concentrations of glutamate can result in single-channel currents that show abrupt changes in open probability ('modal activity') (Prieto and Wollmuth, 2010) (**Fig 6**). In their high open probability mode, channels open to the higher conductance levels (including the maximum, O4 level) at a frequency higher than expected from the predicted glutamate occupancy. It therefore seems that this mode displays an increased apparent affinity for glutamate (**Fig 6b**). It has been postulated that the mechanism of this form of modal change is a cooperative interaction between subunits, such that when zero or one of the glutamate binding sites is occupied the channel is in the low open probability mode. When a second binding site is occupied, the third and fourth glutamate molecules then bind rapidly with higher affinity. This would account for an increased open probability and occurrence of O3 and O4 (Prieto and Wollmuth, 2010). This modal switch could arise from a change at the dimer interface following closure of one LBD, or from a change in the non-gated subunits' glutamate affinity or efficacy once the channel has been opened.
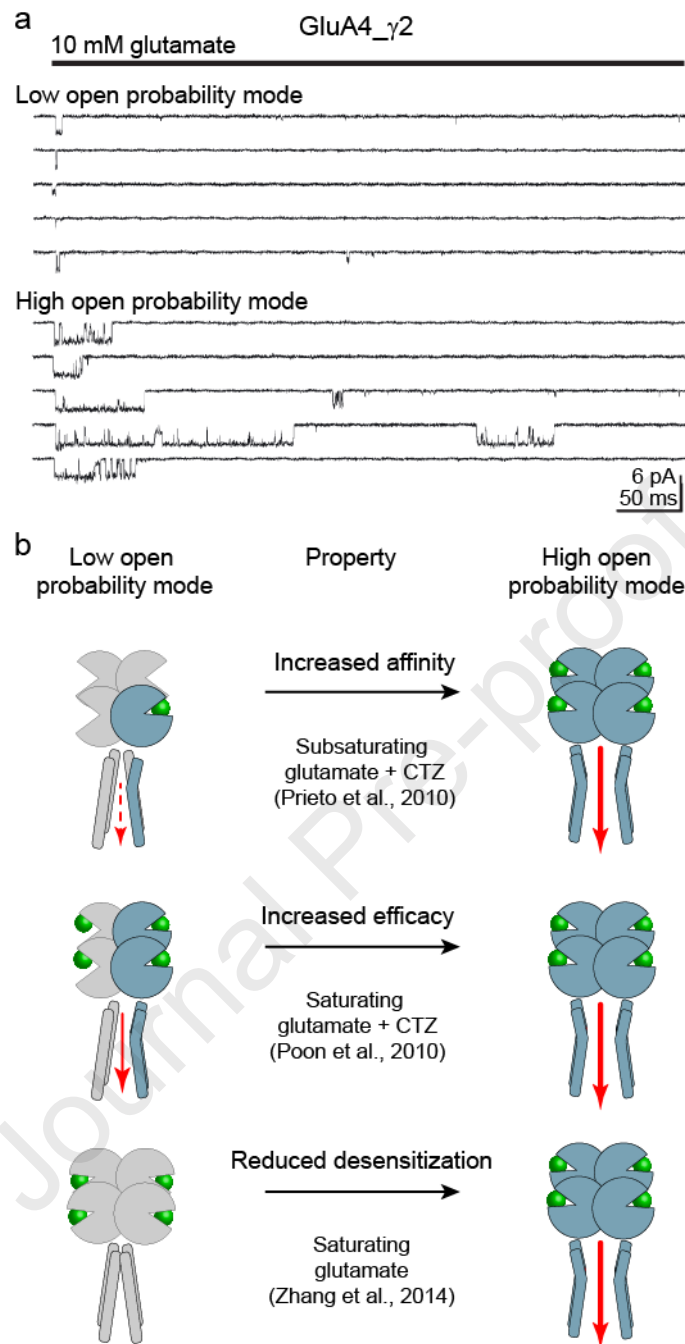
24

Fig 6. AMPAR properties underlying modal activity

a) Selected records from an outside-out patch containing a single GluA4_γ2 tandem receptor. The receptor displayed both the low- (upper traces) and high- (lower traces) open probability modes. Note that when in the high-open probability mode the receptor displayed an increased proportion of higher conductance-level openings together with slowed desensitization. Adapted from Zhang et al. (2014). **b**) Potential properties that could account for the enhanced amplitude and slowed desensitization of single-channel currents seen in the receptor's high-open probability mode. Selected studies documenting each property, along with the experimental conditions used, are indicated below each arrow.

25

While the modal activity identified by (Prieto and Wollmuth, 2010) was apparent on the millisecond timescale, subsequent single-channel studies of homomeric GluA3 receptors identified a separate and complex pattern of five different gating modes (characterized by their different open probabilities), which could last for hundreds of milliseconds or even seconds (Poon et al., 2011; Poon et al., 2010) (**Fig 6b**). The molecular mechanisms underlying these distinct patterns of modal behavior and their stability are still to be determined.

Modal activity in the presence of TARPs: As most native AMPARs are thought to be associated with TARPs, understanding the modal gating of TARP-associated AMPARs is crucial in understanding synaptic transmission. Moding has been identified for GluA4/γ2 and the tandem constructs GluA1_γ2 and GluA4_γ2; these receptors displayed low- and high open probability modes which tended to last for several seconds (Zhang et al., 2014). The high open probability mode was additionally characterized by long openings to the maximum conductance state (**Fig 6a**). Interestingly, the single-channel desensitization kinetics of the low and high open probability modes, correspond well to the fast and slow components of macroscopic desensitization (Cho et al., 2007) (**Fig 6b**). This suggests that normal AMPAR/TARP behaviour reflects a balance between these modes, which is therefore likely to be an important feature of AMPARs within the brain. Indeed, the stark difference between the behaviour of the two modes implies that, if conditions caused a change in the mode favoured by synaptic receptors, it would be sufficient to induce a marked change in synaptic transmission.

Resensitization and superactivation: Certain AMPAR/TARP combinations, in particular those containing γ4, γ7 or γ8, show a slow 'run-up' or 'resensitization' in their steady-state response during prolonged glutamate application (Kato et al., 2010). Under these conditions the single-channel currents arising from GluA2(Q)/γ8 receptors are mediated predominantly by long openings to their maximum conductance state (Carrillo et al., 2020), thus resembling the high open probability channel mode described by Zhang et al. (2014). Furthermore, when γ8-containing- (and γ2-containing-) receptors are activated by trains of brief glutamate pulses, both the peak and steady-state currents show a slow run-up (Carbone and Plested, 2016), suggesting that high frequency synaptic activity may increase the proportion of postsynaptic AMPARs in their high open probability mode. Indeed, there is now good evidence that during repetitive stimulation, a subset of hippocampal synaptic receptors can display resensitization, which enhances their contribution to neuronal excitation (Pampaloni et al., 2021). This form of run-up may depend on an activity-dependent switch to the higher

26

open probability mode, reported by Carbone and Plested (2016) and dubbed 'superactivation'.

TARP structural interactions influencing single-channel modes: During the process of AMPAR activation, movement of the D2 lobes is accompanied by 'vertical' forces on the LBD layer that pull the LBDs closer to the membrane (Durr et al., 2014; Meyerson et al., 2014). For TARPed receptors, this motion is likely to promote engagement of the LBDs with the extracellular loops (especially Ex1) of the associated TARP (Chen et al., 2017). Such an interaction has been proposed to modify the kinetics of channel closure (Dawe et al., 2016; Tomita et al., 2005a; Zhao et al., 2016) and increase agonist efficacy (Chen et al., 2017). In addition, it appears that TARPs can also influence AMPAR behavior by interacting with the LBD-TM linkers (Riva et al., 2017) and the TM domains (Soto et al., 2014). Interestingly, there is evidence that the prevalence of the high open probability mode is influenced by TARP stoichiometry within the AMPAR assembly. Thus, the high open probability mode is more prevalent in AMPARs composed of tandem constructs than in AMPARs formed by coexpression of TARPs with GluA subunits (Zhang et al., 2014). This suggests that the phenomenon reflects a concerted action of TARPs on AMPARs, being more prominent in fully TARPed receptors, which is also consistent with the observation from noise analysis that only fully TARP-saturated GluA1 homomers display an increased conductance (Miguez-Cabello et al., 2020).

Similarly, resensitization/superactivation, which may reflect a seconds long increase in the proportion of channels entering their high open probability mode, is more evident in AMPAR complexes that contain the maximum number of TARPs (Carbone and Plested, 2016). The phenomenon is particularly apparent for AMPARs containing TARP γ8 (Carbone and Plested, 2016; Kato et al., 2010) which display long single-channel openings to the highest conductance level at steady-state (**See Fig 1e**) (Carrillo et al., 2020). It is therefore of note that γ8 contains a long Ex1 extracellular loop. Compared with other TARPs this allows it to interact more extensively with the lower lobe of the LBD (and potentially with the upper lobe), which may stabilize the gated receptor (Herguedas et al., 2019). However, γ7, which has a shorter Ex1 loop than other TARPs, also gives rise to AMPARs that display resensitization (Kato et al., 2010) suggesting other factors are also important.

Conclusions

Single-channel studies have added to our understanding of the kinetic, conductance and pharmacological properties of AMPARs. They have established that channel properties depend critically on the receptor's subunit composition, are regulated by post-transcriptional

RNA editing, and are altered by post-translational modification. However, functional diversity is not controlled purely by the pore-forming subunits. Assembly, trafficking, and functional heterogeneity of AMPAR channels also depend on a repertoire of associated auxiliary subunits, a feature that is particularly striking for these receptors. The pore forming subunits and their auxiliary proteins are the primary elements involved in information transfer and storage in the brain, and undergo rapid change during synaptic plasticity, through alteration in their number, subunit composition, protein partner interactions, or phosphorylation state. Single-channel studies are continuing to provide unique insight into the functional face of the AMPAR channels and their involvement in these processes. When placed in the context of elegant structural studies, this is providing an increasingly clear picture of the operation, diversity and plasticity of these vital receptors.

Competing interests' statement: The authors have no competing interests to declare

Author contributions: Both authors made substantial contributions to the writing of the article, revising critically for important intellectual content, and approval of the final Submitted version.

References

Amin, J.B., Leng, X., Gochman, A., Zhou, H.X., and Wollmuth, L.P. (2018). A conserved glycine harboring disease-associated mutations permits NMDA receptor slow deactivation and high Ca(2+) permeability. Nat Commun *9*, 3748.

Armstrong, N., and Gouaux, E. (2000). Mechanisms for activation and antagonism of an AMPA-sensitive glutamate receptor: crystal structures of the GluR2 ligand binding core. Neuron *28*, 165-181.

Armstrong, N., Jasti, J., Beich-Frandsen, M., and Gouaux, E. (2006). Measurement of conformational changes accompanying desensitization in an ionotropic glutamate receptor. Cell *127*, 85-97.

Banke, T.G., Bowie, D., Lee, H., Huganir, R.L., Schousboe, A., and Traynelis, S.F. (2000). Control of GluR1 AMPA receptor function by cAMP-dependent protein kinase. J Neurosci *20*, 89-102.

Barria, A., Derkach, V., and Soderling, T. (1997). Identification of the Ca2+/calmodulin-dependent protein kinase II regulatory phosphorylation site in the alpha-amino-3-hydroxyl-5-methyl-4-isoxazole-propionate-type glutamate receptor. J Biol Chem *272*, 32727-32730.

Bats, C., Groc, L., and Choquet, D. (2007). The interaction between Stargazin and PSD-95 regulates AMPA receptor surface trafficking. Neuron *53*, 719-734.

Bowie, D., and Lange, G.D. (2002). Functional stoichiometry of glutamate receptor desensitization. J Neurosci *22*, 3392-3403.

Bowie, D., and Mayer, M.L. (1995). Inward rectification of both AMPA and kainate subtype glutamate receptors generated by polyamine-mediated ion channel block. Neuron *15*, 453-462.

Burnashev, N., Villarroel, A., and Sakmann, B. (1996). Dimensions and ion selectivity of recombinant AMPA and kainate receptor channels and their dependence on Q/R site residues. J Physiol *496 (Pt 1)*, 165-173.

Carbone, A.L., and Plested, A.J. (2016). Superactivation of AMPA receptors by auxiliary proteins. Nat Commun *7*, 10178.

Carrillo, E., Shaikh, S.A., Berka, V., Durham, R.J., Litwin, D.B., Lee, G., MacLean, D.M., Nowak, L.M., and Jayaraman, V. (2020). Mechanism of modulation of AMPA receptors by TARP-gamma8. J Gen Physiol *152*.

Chen, L., Chetkovich, D.M., Petralia, R.S., Sweeney, N.T., Kawasaki, Y., Wenthold, R.J., Bredt, D.S., and Nicoll, R.A. (2000). Stargazin regulates synaptic targeting of AMPA receptors by two distinct mechanisms. Nature *408*, 936-943.

Chen, S., and Gouaux, E. (2019). Structure and mechanism of AMPA receptor - auxiliary protein complexes. Curr Opin Struct Biol *54*, 104-111.

Chen, S., Zhao, Y., Wang, Y., Shekhar, M., Tajkhorshid, E., and Gouaux, E. (2017). Activation and Desensitization Mechanism of AMPA Receptor-TARP Complex by Cryo-EM. Cell *170*, 1234-1246 e1214.

Cho, C.H., St-Gelais, F., Zhang, W., Tomita, S., and Howe, J.R. (2007). Two families of TARP isoforms that have distinct effects on the kinetic properties of AMPA receptors and synaptic currents. Neuron *55*, 890-904.

Coombs, I.D., MacLean, D.M., Jayaraman, V., Farrant, M., and Cull-Candy, S.G. (2017). Dual Effects of TARP gamma-2 on Glutamate Efficacy Can Account for AMPA Receptor Autoinactivation. Cell Rep *20*, 1123-1135.

Coombs, I.D., Soto, D., McGee, T.P., Gold, M.G., Farrant, M., and Cull-Candy, S.G. (2019). Homomeric GluA2(R) AMPA receptors can conduct when desensitized. Nat Commun *10*, 4312.

Coombs, I.D., Soto, D., Zonouzi, M., Renzi, M., Shelley, C., Farrant, M., and Cull-Candy, S.G. (2012). Cornichons modify channel properties of recombinant and glial AMPA receptors. J Neurosci *32*, 9796-9804.

Cull-Candy, S.G., Howe, J.R., and Ogden, D.C. (1988). Noise and single channels activated by excitatory amino acids in rat cerebellar granule neurones. J Physiol *400*, 189-222.

Cull-Candy, S.G., and Usowicz, M.M. (1987). Multiple-conductance channels activated by excitatory amino acids in cerebellar neurons. Nature *325*, 525-528.

Cull-Candy, S.G., and Usowicz, M.M. (1989). On the multiple-conductance single channels activated by excitatory amino acids in large cerebellar neurones of the rat. J Physiol *415*, 555-582.

Dawe, G.B., Musgaard, M., Aurousseau, M.R.P., Nayeem, N., Green, T., Biggin, P.C., and Bowie, D. (2016). Distinct Structural Pathways Coordinate the Activation of AMPA Receptor-Auxiliary Subunit Complexes. Neuron *89*, 1264-1276.

Del Castillo, J., and Katz, B. (1957). Interaction at end-plate receptors between different choline derivatives. Proc R Soc Lond B Biol Sci *146*, 369-381.

Derkach, V., Barria, A., and Soderling, T.R. (1999). Ca2+/calmodulin-kinase II enhances channel conductance of alpha-amino-3-hydroxy-5-methyl-4-isoxazolepropionate type glutamate receptors. Proc Natl Acad Sci U S A *96*, 3269-3274.

Diaz-Alonso, J., Morishita, W., Incontro, S., Simms, J., Holtzman, J., Gill, M., Mucke, L., Malenka, R.C., and Nicoll, R.A. (2020). Long-term potentiation is independent of the C-tail of the GluA1 AMPA receptor subunit. Elife *9*.

Diering, G.H., and Huganir, R.L. (2018). The AMPA Receptor Code of Synaptic Plasticity. Neuron *100*, 314-329.

Donevan, S.D., and Rogawski, M.A. (1993). GYKI 52466, a 2,3-benzodiazepine, is a highly selective, noncompetitive antagonist of AMPA/kainate receptor responses. Neuron *10*, 51-59.

Durr, K.L., Chen, L., Stein, R.A., De Zorzi, R., Folea, I.M., Walz, T., McHaourab, H.S., and Gouaux, E. (2014). Structure and dynamics of AMPA receptor GluA2 in resting, pre-open, and desensitized states. Cell *158*, 778-792.

Esteban, J.A., Shi, S.H., Wilson, C., Nuriya, M., Huganir, R.L., and Malinow, R. (2003). PKA phosphorylation of AMPA receptor subunits controls synaptic trafficking underlying plasticity. Nat Neurosci *6*, 136-143.

Fucile, S., Miledi, R., and Eusebi, F. (2006). Effects of cyclothiazide on GluR1/AMPA receptors. Proc Natl Acad Sci U S A *103*, 2943-2947.

Gebhardt, C., and Cull-Candy, S.G. (2006). Influence of agonist concentration on AMPA and kainate channels in CA1 pyramidal cells in rat hippocampal slices. J Physiol *573*, 371-394.

Gray, E.E., Guglietta, R., Khakh, B.S., and O'Dell, T.J. (2014). Inhibitory interactions between phosphorylation sites in the C terminus of alpha-Amino-3-hydroxy-5-methyl-4-isoxazolepropionic acid-type glutamate receptor GluA1 subunits. J Biol Chem *289*, 14600-14611.

Greger, I.H., Khatri, L., Kong, X., and Ziff, E.B. (2003). AMPA receptor tetramerization is mediated by Q/R editing. Neuron *40*, 763-774.

Greger, I.H., Watson, J.F., and Cull-Candy, S.G. (2017). Structural and Functional Architecture of AMPA-Type Glutamate Receptors and Their Auxiliary Proteins. Neuron *94*, 713-730.

Gu, X., Mao, X., Lussier, M.P., Hutchison, M.A., Zhou, L., Hamra, F.K., Roche, K.W., and Lu, W. (2016). GSG1L suppresses AMPA receptor-mediated synaptic transmission and uniquely modulates AMPA receptor kinetics in hippocampal neurons. Nat Commun *7*, 10873.

Hayashi, Y., Shi, S.H., Esteban, J.A., Piccini, A., Poncer, J.C., and Malinow, R. (2000). Driving AMPA receptors into synapses by LTP and CaMKII: requirement for GluR1 and PDZ domain interaction. Science *287*, 2262-2267.

Herguedas, B., Watson, J.F., Ho, H., Cais, O., Garcia-Nafria, J., and Greger, I.H. (2019). Architecture of the heteromeric GluA1/2 AMPA receptor in complex with the auxiliary subunit TARP gamma8. Science *364*.

Hibi, S., Ueno, K., Nagato, S., Kawano, K., Ito, K., Norimine, Y., Takenaka, O., Hanada, T., and Yonaga, M. (2012). Discovery of 2-(2-oxo-1-phenyl-5-pyridin-2-yl-1,2-dihydropyridin-3-yl)benzonitrile (perampanel): a novel, noncompetitive alpha-amino-3-hydroxy-5-methyl-4-isoxazolepropanoic acid (AMPA) receptor antagonist. J Med Chem *55*, 10584-10600.

Hollmann, M., Hartley, M., and Heinemann, S. (1991). Ca2+ permeability of KA-AMPA--gated glutamate receptor channels depends on subunit composition. Science *252*, 851-853.

Hollmann, M., and Heinemann, S. (1994). Cloned glutamate receptors. Annu Rev Neurosci *17*, 31-108.

Howe, J.R., Cull-Candy, S.G., and Colquhoun, D. (1991). Currents through single glutamate receptor channels in outside-out patches from rat cerebellar granule cells. J Physiol *432*, 143-202.

Jackson, A.C., Milstein, A.D., Soto, D., Farrant, M., Cull-Candy, S.G., and Nicoll, R.A. (2011). Probing TARP modulation of AMPA receptor conductance with polyamine toxins. J Neurosci *31*, 7511-7520.

Jackson, A.C., and Nicoll, R.A. (2011). The expanding social network of ionotropic glutamate receptors: TARPs and other transmembrane auxiliary subunits. Neuron *70*, 178-199.

Jacobi, E., and von Engelhardt, J. (2021). Modulation of information processing by AMPA receptor auxiliary subunits. J Physiol *599*, 471-483.

Jahr, C.E., and Stevens, C.F. (1987). Glutamate activates multiple single channel conductances in hippocampal neurons. Nature *325*, 522-525.

Jenkins, M.A., Wells, G., Bachman, J., Snyder, J.P., Jenkins, A., Huganir, R.L., Oswald, R.E., and Traynelis, S.F. (2014). Regulation of GluA1 alpha-amino-3-hydroxy-5-methyl-4-isoxazolepropionic acid receptor function by protein kinase C at serine-818 and threonine-840. Mol Pharmacol *85*, 618-629.

Jin, R., Banke, T.G., Mayer, M.L., Traynelis, S.F., and Gouaux, E. (2003). Structural basis for partial agonist action at ionotropic glutamate receptors. Nat Neurosci *6*, 803-810.

Kamboj, S.K., Swanson, G.T., and Cull-Candy, S.G. (1995). Intracellular spermine confers rectification on rat calcium-permeable AMPA and kainate receptors. J Physiol *486 (Pt 2)*, 297-303.

Kato, A.S., Gill, M.B., Ho, M.T., Yu, H., Tu, Y., Siuda, E.R., Wang, H., Qian, Y.W., Nisenbaum, E.S., Tomita, S*., et al.* (2010). Hippocampal AMPA receptor gating controlled by both TARP and cornichon proteins. Neuron *68*, 1082-1096.

Kazi, R., Dai, J., Sweeney, C., Zhou, H.X., and Wollmuth, L.P. (2014). Mechanical coupling maintains the fidelity of NMDA receptor-mediated currents. Nat Neurosci *17*, 914-922.

Keinanen, K., Wisden, W., Sommer, B., Werner, P., Herb, A., Verdoorn, T.A., Sakmann, B., and Seeburg, P.H. (1990). A family of AMPA-selective glutamate receptors. Science *249*, 556-560.

Khodosevich, K., Jacobi, E., Farrow, P., Schulmann, A., Rusu, A., Zhang, L., Sprengel, R., Monyer, H., and von Engelhardt, J. (2014). Coexpressed auxiliary subunits exhibit distinct modulatory profiles on AMPA receptor function. Neuron *83*, 601-615.

Klaassen, R.V., Stroeder, J., Coussen, F., Hafner, A.S., Petersen, J.D., Renancio, C., Schmitz, L.J., Normand, E., Lodder, J.C., Rotaru, D.C*., et al.* (2016). Shisa6 traps AMPA receptors at postsynaptic sites and prevents their desensitization during synaptic activity. Nat Commun *7*, 10682.

Koh, D.S., Burnashev, N., and Jonas, P. (1995). Block of native Ca(2+)-permeable AMPA receptors in rat brain by intracellular polyamines generates double rectification. J Physiol *486 (Pt 2)*, 305-312.

Kristensen, A.S., Jenkins, M.A., Banke, T.G., Schousboe, A., Makino, Y., Johnson, R.C., Huganir, R., and Traynelis, S.F. (2011). Mechanism of Ca2+/calmodulin-dependent kinase II regulation of AMPA receptor gating. Nat Neurosci *14*, 727-735.

Lee, H.K., Takamiya, K., Han, J.S., Man, H., Kim, C.H., Rumbaugh, G., Yu, S., Ding, L., He, C., Petralia, R.S*., et al.* (2003). Phosphorylation of the AMPA receptor GluR1 subunit is required for synaptic plasticity and retention of spatial memory. Cell *112*, 631-643.

Lee, H.K., Takamiya, K., Kameyama, K., He, K., Yu, S., Rossetti, L., Wilen, D., and Huganir, R.L. (2007). Identification and characterization of a novel phosphorylation site on the GluR1 subunit of AMPA receptors. Mol Cell Neurosci *36*, 86-94.

Lin, D.T., Makino, Y., Sharma, K., Hayashi, T., Neve, R., Takamiya, K., and Huganir, R.L. (2009). Regulation of AMPA receptor extrasynaptic insertion by 4.1N, phosphorylation and palmitoylation. Nat Neurosci *12*, 879-887.

MacLean, D.M., Ramaswamy, S.S., Du, M., Howe, J.R., and Jayaraman, V. (2014). Stargazin promotes closure of the AMPA receptor ligand-binding domain. J Gen Physiol *144*, 503-512.

McGee, T.P., Bats, C., Farrant, M., and Cull-Candy, S.G. (2015). Auxiliary Subunit GSG1L Acts to Suppress Calcium-Permeable AMPA Receptor Function. J Neurosci *35*, 16171-16179.

Menuz, K., Stroud, R.M., Nicoll, R.A., and Hays, F.A. (2007). TARP auxiliary subunits switch AMPA receptor antagonists into partial agonists. Science *318*, 815-817.

Meyerson, J.R., Kumar, J., Chittori, S., Rao, P., Pierson, J., Bartesaghi, A., Mayer, M.L., and Subramaniam, S. (2014). Structural mechanism of glutamate receptor activation and desensitization. Nature *514*, 328-334.

Miguez-Cabello, F., Sanchez-Fernandez, N., Yefimenko, N., Gasull, X., Gratacos-Batlle, E., and Soto, D. (2020). AMPAR/TARP stoichiometry differentially modulates channel properties. Elife *9*.

Momiyama, A., Silver, R.A., Hausser, M., Notomi, T., Wu, Y., Shigemoto, R., and Cull-Candy, S.G. (2003). The density of AMPA receptors activated by a transmitter quantum at the climbing fibre-Purkinje cell synapse in immature rats. J Physiol *549*, 75-92.

Morimoto-Tomita, M., Zhang, W., Straub, C., Cho, C.H., Kim, K.S., Howe, J.R., and Tomita, S. (2009). Autoinactivation of neuronal AMPA receptors via glutamate-regulated TARP interaction. Neuron *61*, 101-112.

Nakagawa, T. (2019). Structures of the AMPA receptor in complex with its auxiliary subunit cornichon. Science *366*, 1259-1263.

Oh, M.C., and Derkach, V.A. (2005). Dominant role of the GluR2 subunit in regulation of AMPA receptors by CaMKII. Nat Neurosci *8*, 853-854.

Pampaloni, N.P., Riva, I., Carbone, A.L., and Plested, A.J.R. (2021). Slow AMPA receptors in hippocampal principal cells. Cell Rep *36*, 109496.

Patneau, D.K., and Mayer, M.L. (1990). Structure-activity relationships for amino acid transmitter candidates acting at N-methyl-D-aspartate and quisqualate receptors. J Neurosci *10*, 2385-2399.

Plested, A.J., and Mayer, M.L. (2009). AMPA receptor ligand binding domain mobility revealed by functional cross linking. J Neurosci *29*, 11912-11923.

Poon, K., Ahmed, A.H., Nowak, L.M., and Oswald, R.E. (2011). Mechanisms of modal activation of GluA3 receptors. Mol Pharmacol *80*, 49-59.

Poon, K., Nowak, L.M., and Oswald, R.E. (2010). Characterizing single-channel behavior of GluA3 receptors. Biophys J *99*, 1437-1446.

Prieto, M.L., and Wollmuth, L.P. (2010). Gating modes in AMPA receptors. J Neurosci *30*, 4449-4459.

Riva, I., Eibl, C., Volkmer, R., Carbone, A.L., and Plested, A.J. (2017). Control of AMPA receptor activity by the extracellular loops of auxiliary proteins. Elife *6*.

Roche, K.W., O'Brien, R.J., Mammen, A.L., Bernhardt, J., and Huganir, R.L. (1996). Characterization of multiple phosphorylation sites on the AMPA receptor GluR1 subunit. Neuron *16*, 1179-1188.

Rosenmund, C., Stern-Bach, Y., and Stevens, C.F. (1998). The tetrameric structure of a glutamate receptor channel. Science *280*, 1596-1599.

Rossmann, M., Sukumaran, M., Penn, A.C., Veprintsev, D.B., Babu, M.M., and Greger, I.H. (2011). Subunit-selective N-terminal domain associations organize the formation of AMPA receptor heteromers. EMBO J *30*, 959-971.

Schwenk, J., Baehrens, D., Haupt, A., Bildl, W., Boudkkazi, S., Roeper, J., Fakler, B., and Schulte, U. (2014). Regional diversity and developmental dynamics of the AMPA-receptor proteome in the mammalian brain. Neuron *84*, 41-54.

Schwenk, J., Boudkkazi, S., Kocylowski, M.K., Brechet, A., Zolles, G., Bus, T., Costa, K., Kollewe, A., Jordan, J., Bank, J.*, et al.* (2019). An ER Assembly Line of AMPA-Receptors Controls Excitatory Neurotransmission and Its Plasticity. Neuron *104*, 680-692 e689.

Schwenk, J., Harmel, N., Brechet, A., Zolles, G., Berkefeld, H., Muller, C.S., Bildl, W., Baehrens, D., Huber, B., Kulik, A.*, et al.* (2012). High-resolution proteomics unravel architecture and molecular diversity of native AMPA receptor complexes. Neuron *74*, 621-633.

Schwenk, J., Harmel, N., Zolles, G., Bildl, W., Kulik, A., Heimrich, B., Chisaka, O., Jonas, P., Schulte, U., Fakler, B.*, et al.* (2009). Functional proteomics identify cornichon proteins as auxiliary subunits of AMPA receptors. Science *323*, 1313-1319.

Seeburg, P.H., and Hartner, J. (2003). Regulation of ion channel/neurotransmitter receptor function by RNA editing. Curr Opin Neurobiol *13*, 279-283.

Shanks, N.F., Savas, J.N., Maruo, T., Cais, O., Hirao, A., Oe, S., Ghosh, A., Noda, Y., Greger, I.H., Yates, J.R., 3rd*, et al.* (2012). Differences in AMPA and kainate receptor interactomes facilitate identification of AMPA receptor auxiliary subunit GSG1L. Cell Rep *1*, 590-598.

Shelley, C., Farrant, M., and Cull-Candy, S.G. (2012). TARP-associated AMPA receptors display an increased maximum channel conductance and multiple kinetically distinct open states. J Physiol *590*, 5723-5738.

Shi, E.Y., Yuan, C.L., Sipple, M.T., Srinivasan, J., Ptak, C.P., Oswald, R.E., and Nowak, L.M. (2019). Noncompetitive antagonists induce cooperative AMPA receptor channel gating. J Gen Physiol *151*, 156-173.

Shi, S., Hayashi, Y., Esteban, J.A., and Malinow, R. (2001). Subunit-specific rules governing AMPA receptor trafficking to synapses in hippocampal pyramidal neurons. Cell *105*, 331-343.

Smith, T.C., and Howe, J.R. (2000). Concentration-dependent substate behavior of native AMPA receptors. Nat Neurosci *3*, 992-997.

Smith, T.C., Wang, L.Y., and Howe, J.R. (2000). Heterogeneous conductance levels of native AMPA receptors. J Neurosci *20*, 2073-2085.

Sobolevsky, A.I., Rosconi, M.P., and Gouaux, E. (2009). X-ray structure, symmetry and mechanism of an AMPA-subtype glutamate receptor. Nature *462*, 745-756.

Sommer, B., Kohler, M., Sprengel, R., and Seeburg, P.H. (1991). RNA editing in brain controls a determinant of ion flow in glutamate-gated channels. Cell *67*, 11-19.

Soto, D., Coombs, I.D., Gratacos-Batlle, E., Farrant, M., and Cull-Candy, S.G. (2014). Molecular mechanisms contributing to TARP regulation of channel conductance and polyamine block of calcium-permeable AMPA receptors. J Neurosci *34*, 11673-11683.

Soto, D., Coombs, I.D., Kelly, L., Farrant, M., and Cull-Candy, S.G. (2007). Stargazin attenuates intracellular polyamine block of calcium-permeable AMPA receptors. Nat Neurosci *10*, 1260-1267.

Sun, Y., Olson, R., Horning, M., Armstrong, N., Mayer, M., and Gouaux, E. (2002). Mechanism of glutamate receptor desensitization. Nature *417*, 245-253.

Swanson, G.T., Kamboj, S.K., and Cull-Candy, S.G. (1997). Single-channel properties of recombinant AMPA receptors depend on RNA editing, splice variation, and subunit composition. J Neurosci *17*, 58-69.

Tomita, S., Adesnik, H., Sekiguchi, M., Zhang, W., Wada, K., Howe, J.R., Nicoll, R.A., and Bredt, D.S. (2005a). Stargazin modulates AMPA receptor gating and trafficking by distinct domains. Nature *435*, 1052-1058.

Tomita, S., Chen, L., Kawasaki, Y., Petralia, R.S., Wenthold, R.J., Nicoll, R.A., and Bredt, D.S. (2003). Functional studies and distribution define a family of transmembrane AMPA receptor regulatory proteins. J Cell Biol *161*, 805-816.

Tomita, S., Stein, V., Stocker, T.J., Nicoll, R.A., and Bredt, D.S. (2005b). Bidirectional synaptic plasticity regulated by phosphorylation of stargazin-like TARPs. Neuron *45*, 269-277.

Traynelis, S.F., Wollmuth, L.P., McBain, C.J., Menniti, F.S., Vance, K.M., Ogden, K.K., Hansen, K.B., Yuan, H., Myers, S.J., and Dingledine, R. (2010). Glutamate receptor ion channels: structure, regulation, and function. Pharmacological reviews *62*, 405-496.

Twomey, E.C., Yelshanskaya, M.V., Grassucci, R.A., Frank, J., and Sobolevsky, A.I. (2017a). Channel opening and gating mechanism in AMPA-subtype glutamate receptors. Nature *549*, 60-65.

Twomey, E.C., Yelshanskaya, M.V., Grassucci, R.A., Frank, J., and Sobolevsky, A.I. (2017b). Structural Bases of Desensitization in AMPA Receptor-Auxiliary Subunit Complexes. Neuron *94*, 569-580 e565.

Usowicz, M.M., Gallo, V., and Cull-Candy, S.G. (1989). Multiple conductance channels in type-2 cerebellar astrocytes activated by excitatory amino acids. Nature *339*, 380-383.

von Engelhardt, J., Mack, V., Sprengel, R., Kavenstock, N., Li, K.W., Stern-Bach, Y., Smit, A.B., Seeburg, P.H., and Monyer, H. (2010). CKAMP44: a brain-specific protein attenuating short-term synaptic plasticity in the dentate gyrus. Science *327*, 1518-1522.

Wilding, T.J., Chen, K., and Huettner, J.E. (2010). Fatty acid modulation and polyamine block of GluK2 kainate receptors analyzed by scanning mutagenesis. J Gen Physiol *136*, 339-352.

33

Wyllie, D.J., and Cull-Candy, S.G. (1994). A comparison of non-NMDA receptor channels in type-2 astrocytes and granule cells from rat cerebellum. J Physiol *475*, 95-114.

Wyllie, D.J., Traynelis, S.F., and Cull-Candy, S.G. (1993). Evidence for more than one type of non-NMDA receptor in outside-out patches from cerebellar granule cells of the rat. J Physiol *463*, 193-226.

Yelshanskaya, M.V., Singh, A.K., Sampson, J.M., Narangoda, C., Kurnikova, M., and Sobolevsky, A.I. (2016). Structural Bases of Noncompetitive Inhibition of AMPA-Subtype Ionotropic Glutamate Receptors by Antiepileptic Drugs. Neuron *91*, 1305-1315.

Yu, J., Rao, P., Clark, S., Mitra, J., Ha, T., and Gouaux, E. (2021). Hippocampal AMPA receptor assemblies and mechanism of allosteric inhibition. Nature.

Yuan, C.L., Shi, E.Y., Srinivasan, J., Ptak, C.P., Oswald, R.E., and Nowak, L.M. (2019). Modulation of AMPA Receptor Gating by the Anticonvulsant Drug, Perampanel. ACS Med Chem Lett *10*, 237-242.

Zhang, D., Watson, J.F., Matthews, P.M., Cais, O., and Greger, I.H. (2021). Gating and modulation of a hetero-octameric AMPA glutamate receptor. Nature.

Zhang, W., Cho, Y., Lolis, E., and Howe, J.R. (2008). Structural and single-channel results indicate that the rates of ligand binding domain closing and opening directly impact AMPA receptor gating. J Neurosci *28*, 932-943.

Zhang, W., Devi, S.P., Tomita, S., and Howe, J.R. (2014). Auxiliary proteins promote modal gating of AMPA- and kainate-type glutamate receptors. Eur J Neurosci *39*, 1138-1147.

Zhang, W., Eibl, C., Weeks, A.M., Riva, I., Li, Y.J., Plested, A.J.R., and Howe, J.R. (2017). Unitary Properties of AMPA Receptors with Reduced Desensitization. Biophys J *113*, 2218-2235.

Zhao, H., Berger, A.J., Brown, P.H., Kumar, J., Balbo, A., May, C.A., Casillas, E., Jr., Laue, T.M., Patterson, G.H., Mayer, M.L.*, et al.* (2012). Analysis of high-affinity assembly for AMPA receptor amino-terminal domains. J Gen Physiol *139*, 371-388.

Zhao, Y., Chen, S., Swensen, A.C., Qian, W.J., and Gouaux, E. (2019). Architecture and subunit arrangement of native AMPA receptors elucidated by cryo-EM. Science *364*, 355-362.

Zhao, Y., Chen, S., Yoshioka, C., Baconguis, I., and Gouaux, E. (2016). Architecture of fully occupied GluA2 AMPA receptor-TARP complex elucidated by cryo-EM. Nature *536*, 108-111.